Blue-Green Systems

IWA PUBLISHING

250

Blue-Green Systems Vol 2 No 1
doi: 10.2166/bgs.2020.101

Detention-based green roofs for stormwater management under extreme precipitation due to climate change

Vladimír Hamouz[a,*], Vincent Pons[a], Edvard Sivertsen[b], Gema Sakti Raspati[b], Jean-Luc Bertrand-Krajewski[c] and Tone Merete Muthanna[a]

[a] Department of Civil and Environmental Engineering, Norwegian University of Science and Technology (NTNU), N-7491 Trondheim, Norway

[b] SINTEF AS, S.P. Andersens veg 3, N-7465 Trondheim, Norway

[c] Université de Lyon, INSA Lyon, DEEP (EA 7429), 11 rue de la Physique, F- 69621, Villeurbanne cedex, France

*Corresponding author. E-mail: vladimir.hamouz@ntnu.no

Abstract

Rooftops cover a large percentage of land area in urban areas, which can potentially be used for stormwater purposes. Seeking adaptation strategies, there is an increasing interest in utilising green roofs for stormwater management. However, the impact of extreme rainfall on the hydrological performance of green roofs and their design implications remain challenging to quantify. In this study, a method was developed to assess the detention performance of a detention-based green roof (underlaid with 100 mm of expanded clay) for current and future climate conditions under extreme precipitation using an artificial rainfall generator. The green roof runoff was found to be more sensitive to the initial water content than the hyetograph shape. The green roof outperformed the black roof in terms of all performance indicators (time of concentration, centroid delay, T50 or peak attenuation). While the time of concentration for the reference black roof was within 5 minutes independently of rainfall intensity, for the green roof was extrapolated between 30 and 90 minutes with intensity from 0.8 to 2.5 mm/min. Adding a layer of expanded clay under the green roof substrate provided a significant improvement to the detention performance under extreme precipitation in current and future climate conditions.

Key words: 20-year return period, climate change, depth duration frequency curves, design rainfall, detention-based green roofs, performance indicators

Highlights

- A method to assess the performance of a green roof under extreme events with a rainfall simulator was developed.
- Underlying a thin extensive green roof with expanded clay provided significant improvement to the detention performance.
- The study demonstrated that extensive green roofs with an added detention layer can have an effect also for extreme precipitation events including a climate factor.
- New knowledge on the water distribution within the roof from antecedent precipitation and how it affects the future performance.
- Demonstrating that the runoff can be predicted from the initial moisture, showing that for this roof the runoff exponentially increased with increasing initial moisture.

Blue-Green Systems Vol 2 No 1
doi: 10.2166/bgs.2020.101

Graphical Abstract

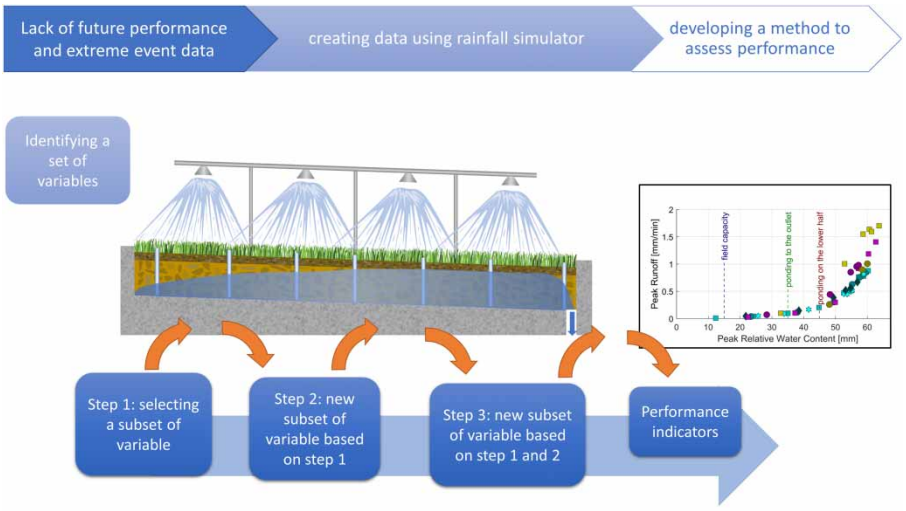

INTRODUCTION

Climate change is increasing the exposure and vulnerability of urban environments to local flooding (among others: (Few 2003; Miller & Hutchins 2017; Hettiarachchi *et al.* 2018). The increasing frequency of extreme precipitation and growing urbanization have amplified the need for sustainable design and management of stormwater measures in urban areas (Mentens *et al.* 2006; Arnbjerg-Nielsen *et al.* 2013; Zhou 2014). Consequently, green roofs have become a common and popular green infrastructure solution around the world (Stovin 2010; Voyde *et al.* 2010; Fassman-Beck *et al.* 2013). The use of green roofs as a stormwater solution is rapidly growing across the Nordic countries, and several municipalities have set targets for their implementation (Copenhagen 2011).

Norway has adopted a three-step approach to stormwater management, where step 1 aims to infiltrate all small events onsite (a well-established and effective solution to reduce peak runoff from impervious surfaces), step 2 aims to safely detain all medium-size events, while step 3 aims to ensure safe floodways for all extreme events (Lindholm *et al.* 2008). Green roofs target events covering both step 1 and step 2. Although there is no infiltration into the ground from green roofs, the small events typically do not generate runoff from the roofs as the water is retained in the substrate and later released through evapotranspiration. Small to medium events are both partly retained in the roof and partly detained and released as delayed runoff. Recently, a new research dealing with a lightweight expanded clay-based roof (also called grey roof) has demonstrated the potential to attenuate intense rainfalls (Hamouz *et al.* 2018). However, little research has been conducted on the performance of green and grey roofs during extreme events. Extreme events, by their nature, occur neither regularly nor frequently, and they are therefore difficult to capture. Additionally, due to climate change, extreme events are expected to increase in intensity and frequency (Stocker 2014; Hanssen-Bauer *et al.* 2017; Hoegh-Guldberg *et al.* 2018). A great amount of uncertainty is linked to the change in extreme events as the trajectory of climate change itself remains uncertain. This is why several scenarios depending on impact of human activities on climate have been developed to evaluate and predict this change (Hanssen-Bauer *et al.* 2017).

Green roofs offer stormwater solutions that can conceivably contribute to the management of extreme events as they allow the opportunity to deal with stormwater directly at the source. The critical performance provided by green roofs is their retention and detention capacity. Detention performance is principally related to runoff delay, attenuation, and peak flow reduction (Stovin *et al.* 2017; Hamouz *et al.* 2018) which are crucial to dealing with extreme events since retention capacities are limited

Blue-Green Systems Vol 2 No 1
doi: 10.2166/bgs.2020.101

during extreme precipitation (VanWoert *et al.* 2005; Villarreal & Bengtsson 2005; Speak *et al.* 2013; Johannessen *et al.* 2018). The use of a combined solution comprised of both green and expanded clay-based (grey) elements is expected to provide a way to design a structure able to achieve long-term retention and event-based detention performance capable of dealing with both conventional and extreme events. There is a consensus in the -literature that the performance of green roofs is subject to local weather patterns (Berndtsson 2010; Li & Babcock 2014; Stovin *et al.* 2017). Common practices to study the performance of green roofs under various locations rely on: field studies limited by available data and location, and modelling studies limited by available data and the transferability of the model (Johannessen *et al.* 2019). The assessment of detention performance can be challenging due to the irregularity of natural precipitation patterns and the variable storage capacity available at the time of a given precipitation event (Stovin *et al.* 2017). Due to the difficulties involved with identifying detention metrics that describe the performance of green roofs for natural precipitation and lack of data on extreme rainfall events, the use of a rainfall simulator was found to be an effective method for testing the roof under extreme 'input-controlled' (e.g. hyetograph and initial water content) variables and evaluating the roof performance. Artificial rain has already been used to simulate various hyetographs to deal with lack of data associated with intense rain (Bengtsson 2005; Villarreal & Bengtsson 2005). Spatial uniformity of the simulated rainfall has been investigated in a certain number of studies (Naves *et al.* 2017; Naves *et al.* 2019). However, no research was found to apply the rainfall simulator to test different hyetographs on a full-scale green roof under changing initial climate conditions.

As a green roof's performance is dependent on water content, the use of a rainfall simulator might be a solution for controlling storm characteristics and initial conditions, including initial water content for a full-scale roof. Due to the rare occurrence of extreme events, utilising artificial rain is a way to fill the knowledge gap. Therefore, the purpose of this research is to assess a procedure for using artificial rain to study the hydrological performance of a detention-based green roof under extreme events. More precisely, this study focuses on 20-year return period (RP) rain events for three Norwegian cities (Bergen, Oslo, Trondheim), taking into account climate change.

The main objectives of this research were to:

1. Develop a method to test extreme precipitation on a full-scale, detention-based green roof using a rainfall simulator.
2. Assess the hydrological performance of a detention-based green roof under extreme precipitation, exceeding a 20-year return period in current and future conditions and including a 1.4 climate factor.

MATERIALS AND METHODS

The study area

A full-scale field setup was built on top of a roof located approximately 10 meters above ground and 50 meters above sea level. The setup was built to study the hydrological performance of different roof configurations at Høvringen in Trondheim, Norway (63°26′47.5″ N 10°20′11.0″ E). In this paper, a green (underlaid with 100 mm of expanded clay – material characteristics in Appendix, Table A2) (FLL 2008) and a black roof, which both had a total area of 88 m^2 and a longitudinal slope of 2%, were considered (Figure 1). More information about the field setup may be found in previous studies (Hamouz *et al.* 2018; Hamouz & Muthanna 2019). The detention-based green roof, referred hereafter as the green roof, was tested in this study. The black roof was used as a reference for comparison.

Blue-Green Systems Vol 2 No 1
doi: 10.2166/bgs.2020.101

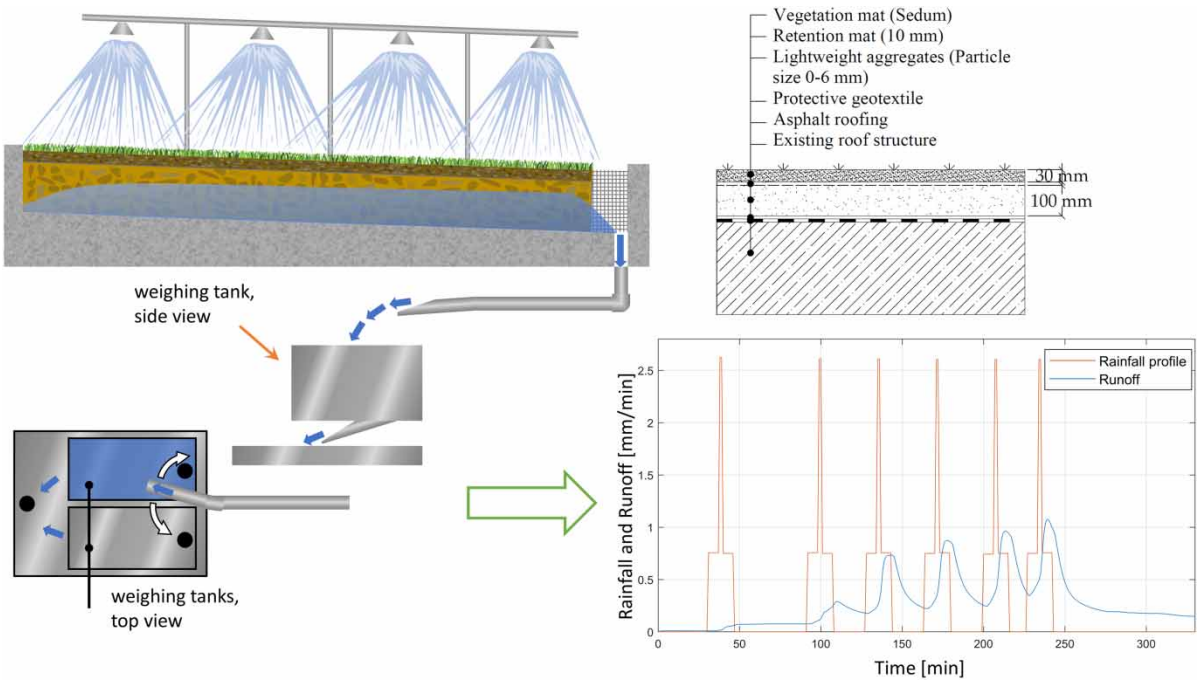

Figure 1 | Conceptual view of the roof, irrigation system and measurement device (on the left), the green roof in a cross-section (on the top right), example of a daily experiment (on the bottom right).

Field data collection

The meteorological and experimental data were collected during a period lasting from May 2019 to October 2019. Natural precipitation was measured by a heated tipping bucket rain gauge (Lambrecht meteo GmbH 1518 H3, Lambrecht meteo GmbH, Göttingen, Germany) with a resolution of 0.1 mm at 1-min intervals and with an uncertainty of $\pm 2\%$. Runoff was measured using a weight-based system (accuracy class C3 according to OIML R60) with two tanks located downstream of the drainage outlet (a 110 mm pipe). All data were recorded at 1-min intervals using a CR 1000 data logger (Campbell Scientific, Inc.). More information related to the instrumentation may be found in other studies (Hamouz *et al.* 2018; Hamouz & Muthanna 2019). Additionally, eight plexiglass tubes were buried vertically along the longitudinal edge of the roof for visual observation and estimation of spatial water distribution within the roof at the beginning and the end of each individual event during the tests.

Rainfall simulator and future climate scenarios

The field site was equipped with a setup using a grid of non-regulated nozzles (4 nozzles per line, 4 lines) connected to a water supply pipe that was used to generate the precipitation input. The nozzles were placed 1.5 m above the roof to ensure the maximal spreading effect of water. The enlarged uncertainty (BIPM *et al.* 2009) with respect to the water spatial distribution was $\pm 3\%$. The enlarged uncertainty of inflow was estimated to be ± 0.06 mm/min and caused by variations in inflow (i.e. a pressure drop in the water supply).

The inflow rates were measured by an electromagnetic flowmeter (Siemens Sitrans FM MAG 5000; uncertainty $\pm 0.4\%$ of the flow rate) and regulated using two valves to allow changes of inflow duration and intensity. The decision was made to run rainfalls with different durations, intensities, and inter-event periods (ranging from 5 minutes to more than 74 minutes) to enable different initial water contents (IWC) in the roof and differently shaped hyetographs. The range of intensities (from

Blue-Green Systems Vol 2 No 1
doi: 10.2166/bgs.2020.101

0.8 to 2.5 mm/min) was limited by the minimal flow due to nozzle spread and maximum flow by the capacity of the flow measuring tanks.

Climate change was considered in this study through an increase in precipitation using a climate factor. The Norwegian Climate Centre (https://klimaservicesenter.no/) published recommendations for future short-term precipitation until 2100 (Hanssen-Bauer *et al.* 2017; Dyrrdal & Førland 2019). Based on this recommendation, a 1.4 climatic factor (CF) is advised in Norway. Firstly, precipitation depths for the 20-year return period (RP) were derived from Depth-Duration-Frequency (DDF) curves for three different cities: Bergen (BER), Oslo (OSL), and Trondheim (TRO) (Table 1). The locations were chosen because of their different climatic conditions. Secondly, these DDF curves were multiplied by a climate factor of 1.4 to estimate expected rainfall in the period between 2071 and 2100, including a worst-case scenario with Representative Concentration Pathway (RCP) 8.5 for short-term events. The use of this factor was also suggested in other studies (Kristvik *et al.* 2018; Kristvik *et al.* 2019).

Experimental design

To study the behaviour and performance of the roof under extreme rainfall, four primary variables were identified: (1) IWC (based on water balance) (2) rainfall duration (3) mean intensity of the rainfall and (4) shape of the hyetograph (impact of varying intensity). Additionally, secondary variables (depending on primary variables) were considered: (5) depth of the rainfall, depending on its duration and mean intensity and (6) location and climate change scenario, linking duration and mean intensity using Intensity-Duration-Frequency (IDF) or Depth-Duration-Frequency (DDF) curves.

The main objective was to identify the most significant variables governing the behaviour of the roof. The experimental design has been driven by the Bayesian principle to minimise the number of experiments. This means that the method has been updated by considering the results obtained in the previous steps. The experiments' three main steps were as follows:

1. The first step was conducted to include a primary analysis of the behaviour of the roof. The influence of rainfall intensity was measured by performing the time of concentration (TC) test. The TC was defined as the time for the roof's runoff to equal inflow under constant intensity rainfall. Subsequently, the water drainage was assessed.
2. Based on the results of the first step, the second experiment was conducted to compare the influence on runoff of a change in hyetograph to a change in IWC.
3. Finally, the third step, based on the results of the first two steps, was conducted to study the influence of the duration and intensity while considering the impact of water content (WC).

Step 1: assessing hydrological behaviour of the roof

To fulfil the first step, the green roof TC was estimated for different inflow intensities (0.8, 1.0, 1.2, 1.4, 1.7, 2.0, and 2.5 mm/min) and compared with the black roof TC. The duration of each event was monitored to ensure that both inflow ($\pm$2%) and outflow ($\pm$2%) lay within the boundaries for measurement uncertainty which was set as a threshold for ending the individual tests.

The roof drainage was studied as part of the first step by recording the outflow after the end of the inflow (precipitation) stopped at the conclusion of the TC test. The drainage curves were later updated with the data from steps 2 and 3 to refine the results.

As the performance of the roof depends to a large degree on WC, and given the fact that short, intense rainfalls typically pose the biggest challenge to urban drainage systems, the choice was made to focus on short-duration events by running the rainfalls successively during step2 and 3. Each hyetograph presented below in step 2 and 3 was applied in a sequence separated by dry-periods (from 5 to 74 min). Each hyetograph was repeated 3–9 times (see example Figure 1). The

Table 1 | Summary of the tested rainfall events derived from DDF curves for three locations: Trondheim, Oslo, and Bergen both with and without CF

ID –	Intensity [mm/min]	Depth [mm]	Duration [mm:ss]	Number of blocks [–]	Return Period			Return period CF = 1.4			Notes – –
					TRO [YYYY]	OSL	BER	TRO [YYYY]	OSL	BER	
TRO 1	1.7	12	07:00	9	200	20–25	100	20	5	5–10	–
TRO 2	1.0	16	16:00	8	200	5–10	100	20	2	5	16 min with 1 mm/min intensity
TRO 2a	1.0	16	16:00	7	200	5–10	100	20	2	5	2 min with 2.6 mm/min followed by 14 min with 0.8 mm/min
TRO 2b	1.0	16	16:00	8	200	5–10	100	20	2	5	14 min with 0.8 mm/min followed by 2 min with 2.6 mm/min
TRO 2c	1.0	16	16:00	6	200	5–10	100	20	2	5	7 min with 0.8 mm/min followed by 2 min with 2.6 mm/min and 7 min with 0.8 mm/min
TRO 2d	1.0	16	16:00	6	200	5–10	100	20	2	5	2 min with 2.6 mm/min three times
TRO 3	2.6	9	03:30	9	200	100–200	100	20	10	5–10	–
TRO 4	0.8	20	26:00	6	200	5–10	100	20	2	5	–
OSL 1	1.7	23	16:00	5	>>200	200–> 200	> >200	> 200	20	200– > 200	–
OSL 2	1.0	45	44:00	3	>>200	200–> 200	> >200	> 200	20	200	–
BER 1	1.7	16	09:00	6	> 200	50–100	> 200	50	5–10	20	–
BER 2	1.0	28	23:00	5	> 200	20	> 200	50	5	20	–

Green-shaded areas show the events with 20 RP; the rest was transposed to other locations.

Blue-Green Systems Vol 2 No 1
doi: 10.2166/bgs.2020.101

Blue-Green Systems Vol 2 No 1
doi: 10.2166/bgs.2020.101

inter-event duration was adapted with real-time control of runoff to increase IWC: (1) the peak of runoff had to be reached (2) IWC had to increase (3) the set of IWC had to be evenly distributed.

Step 2: influence of the hyetograph

In the second step, the choice was made to run events with different hyetographs in order to identify to what hyetograph the roof runoff is the most sensitive as well as to assess the significance of the WC in contrast with the hyetograph. In this step, all simulated hyetographs corresponded to the same overall rainfall depth (16 mm) and duration (16 minutes), although with different distributions named TRO 2, 2a, 2b, 2c, and 2d (see Table 1). The duration and intensity were based on the 20-year return period curve of Trondheim with the 1.4 climatic factor.

Step 3: influence of duration and intensity

The third step was split in two sub-steps. Firstly, four events were selected on the 20-year return period curve of Trondheim with the 1.4 climate factor (TRO 1, TRO 2, TRO 3, and TRO 4, see Table 1). Secondly, based on the results of the first sub-step, the list of events was expanded through selecting events from the DDF curves of Bergen and Oslo (Figure 2). The intensities of TRO2 and TRO3 were chosen to select the events and study the influence of the rain duration: two events for Oslo

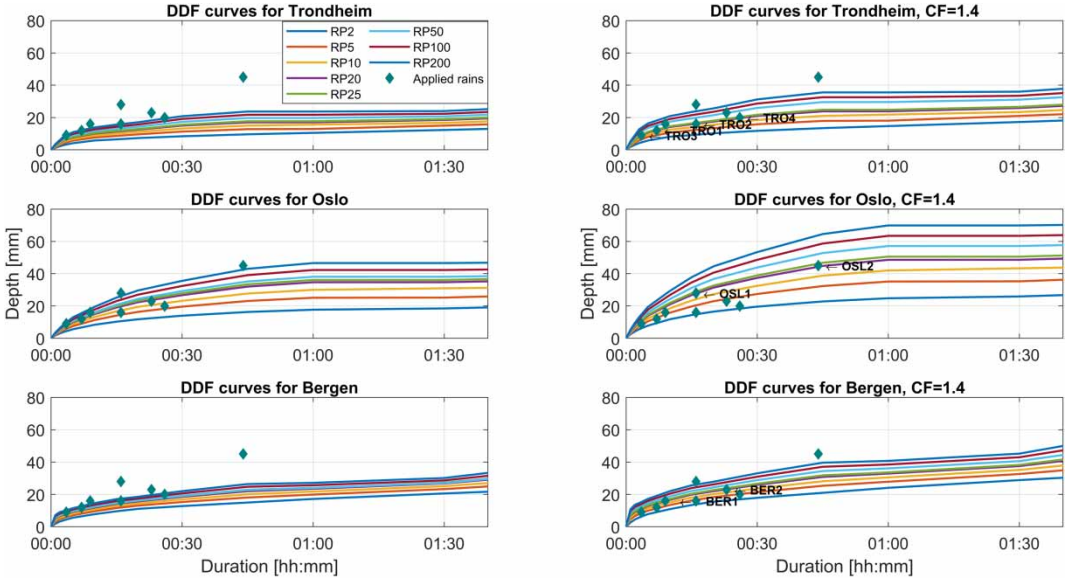

Figure 2 | DDF curves for different return periods, locations, both with (on the right) and without (on the left) the CF of 1.4.

(OSL 1 and OSL 2) and two events for Bergen (BER 1, and BER 2) (Table 1, Table A3, Table A4). An overview of the individual events was plotted for the different locations – both with and without the climatic factor as shown in Figure 2.

Performance indicators and condition indicators

For all simulated rainfall events, a set of performance indicators was estimated:

- *Peak Runoff* $[mm/min]$: maximum runoff at 1 min intervals;
- *Peak Attenuation* $[-] = \dfrac{Peak\ Rainfall - Peak\ Runoff}{Peak\ Rainfall}$ where *Peak Rainfall* $[mm/min]$ is the maximum rainfall intensity at 1 min interval;

Blue-Green Systems Vol 2 No 1
doi: 10.2166/bgs.2020.101

- *Peak Delay* [*min*] - the time between the peak rainfall (the maximum and the last peak when observing multiple peaks) and peak runoff;
- *Centroid Delay* [*min*] - delay between the mass centre of the rainfall and mass centre of the associated runoff;
- *T*50 [*min*] - a delay between 50% of the volume of the rain supplied on the roof and 50% of the volume released out of the roof. *T*50 *delay* was only computable when more than 50% of the rain depth was drained from the roof, whereas *Centroid Delay* and *Peak Delay* rely only on runoff (they do not consider retained water).

Condition indicators:

- *Initial Relative Water Content* [*mm*] – IWC for each event was based on water balance;
- *Peak Relative Water Content* [*mm*] – PRWC Highest value of WC observed before peak runoff. (especially, for constant intensity rainfall it corresponds to the WC at the end of the test).

Data processing

The water balance equation was applied to compute WC within a 1-min time resolution. It was not possible to know the IWC; hence, the WC was computed using the stable tail of the outflow (see section 'Drainage of the roof') as a reference:

$WC_t = WC_{t+1} + R_t - P_t$ *if* $t < t_{ref}$ and $WC_t = WC_{t-1} + R_{t-1} + P_{t-1}$ *if* $t > t_{ref}$ with t_{ref} the daily reference time on the stable tail of the outflow, $\underline{R}$ the runoff, P the rainfall depth and t the time. The unit was kept as mm to facilitate comparison with rainfall depth. The enlarged uncertainty of WC due to water balance was estimated to be ± 0.7 mm based on the Monte Carlo Method. The raw data were analysed using custom MATLAB® scripts.

Due to the short inter-event period between artificial rains, it was not possible to use raw data to compute centroid delay and T50-delay for each rain. Thus, with respect to the first step results, the falling limb between two events was best-fitted using the data from the observed drainage curve. Linear interpolation between successive time intervals was used to minimize the error between the falling limb during dry periods and the roof measured drainage curve. The fitting with the falling limb was evaluated using Nash-Sutcliffe efficiency (NSE). The data from each event was completed to ensure that the outflow volume is equal to the inflow volume and that most of the indicators were computable. Natural precipitation recorded during the experimentation was included in the analysis. However, since the intensity of natural rainfalls was very low compared to the artificial rainfall, the impact of the natural rainfall could be disregarded.

RESULTS AND DISCUSSION

Hydrological analysis of the roof

Time of concentration

To study the behaviour of the roof, the time of concentration (TC), was first assessed. Figure 3 shows the TC curves for different intensities for both the black and the green roofs. TC of the green roof was found inversely proportional to the intensity, i.e. decreasing from 90 minutes to 30 minutes for increasing intensity from 0.8 mm/min to 2.5 mm/min. In contrast, TC of the black roof was found around 5 minutes independently of the intensity. The events defined by their TC and corresponding mean intensity were found to be close or greater than a 200-year return period (RP) event in Trondheim, Bergen and Oslo, having a 1.4 climate factor. The exact TC was challenging to estimate due to

Blue-Green Systems Vol 2 No 1
doi: 10.2166/bgs.2020.101

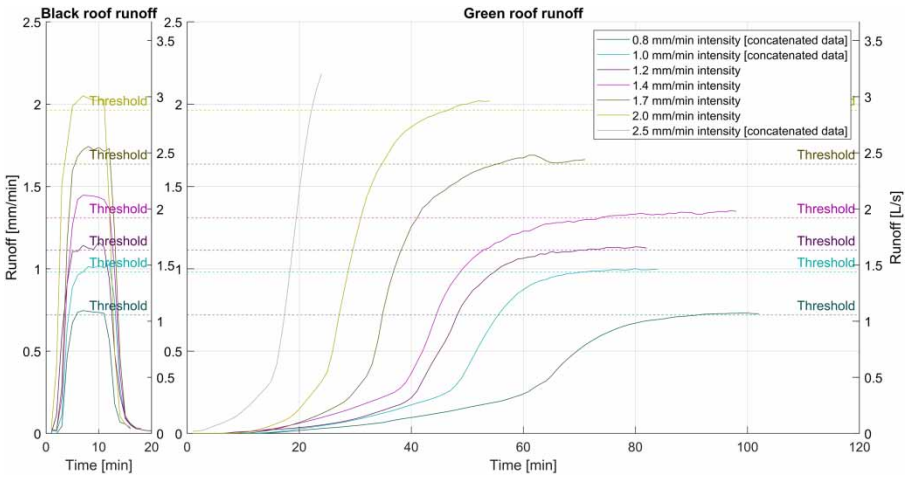

Figure 3 | The TC for different rainfall intensities and rooftop solutions. The TC test for 0.8, 1.0 and 2.5 mm/min intensity started on a partially saturated roof and the curves were completed using concatenation.

its sensitivity to IWC and its slow asymptotic convergence. Moreover, in the 0.8 mm/min and 1.0 mm/min tests, TC was based on concatenation of the runoff, which might have altered the result. Data from concatenation were monitored under different conditions, inner porosity was saturated (inner porosity was hypothesized to distinguish water standing between the aggregates and water stored in the aggregates), which could have led to underestimating TC. The beginning of an event is subject to a transient state (explained later in 'Sensitivity to hyetograph') leading to overestimating TC, even though the transient state was excluded as much as possible. Due to the characteristics of the tested extreme rainfall events, ponding was observed. It was visually inspected that this was linked to the detention properties of the expanded clay and that the outlet was not submerged. Figure 1 shows water distribution in the longitudinal cross section in the middle of the roof.

Dynamic spatial distribution of water within the roof

During all the tests, the spatial distribution of water through the roof longitudinal cross-section was assessed by manual measurement, i.e. the depth of water standing in the roof measured in the 8 plexiglass tubes. This measurement showed the head loss along the flow path toward the outlet. It was found that different distributions of water within the roof for different rainfall events could lead to the same average WC. In addition, it was also observed that, for high WC (more than 35–45 mm of WC), the same average WC could lead to minor differences in outflows (the uncertainty increases with the WC), which is likely linked to different spatial distributions of water within the roof. This

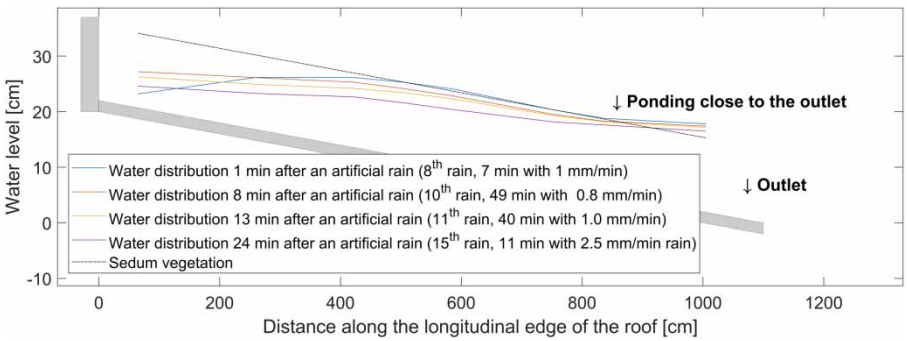

Figure 4 | Cross-section of water distribution in the roof with 50 mm of WC. Data measured during 10.7.2019 along one of the longitudinal edges of the roof. The shaded area (grey) represents the existing concrete structure.

Blue-Green Systems Vol 2 No 1
doi: 10.2166/bgs.2020.101

phenomenon was understood as the dynamic effect linked to both the dual-porosity properties of the detention layer (expanded clay) and the size of the roof as the water cannot be instantly transferred to the outlet. Figure 4 shows that the water distribution within the roof at the end of an artificial rainfall was not linear. It was found, especially in OSL 1, BER 1, and BER 2, that the water distribution was dependent on the rainfall intensity and duration acting as a feedback loop: higher intensity led to higher runoff and greater dynamic effect, leading in turn to higher runoff. In the upper part of the roof (right side of Figure 4), the water level followed a parabolic distribution. During the inter-event period, the water distribution tended to maintain a steady state influenced by gravity and detention properties (the distribution became more linear). Variation of water distribution was explained by capillarity and gravity effect in the detention medium. It was also influenced by both the imperfection of the rainfall simulator (the rainfall spread was not perfectly homogeneous with +/− 3%), and the upper side of the roof having a boundary effect (i.e. close to the top of the roof, no flow was coming from upstream). As well, a different distribution near the outlet would have been expected if the measurement longitudinal cross section aligned with the outlet due to a different boundary condition. It was also hypothesized that inner conductivity (i.e. the aggregates hydraulic conductivity) was lower than the medium hydraulic conductivity. After saturating the medium, the inner porosity was not yet completely saturated. For this reason, it was not found relevant to simplify the behaviour of the roof as initial losses until field capacity was reached and followed by runoff, as these two processes are interconnected.

Drainage of the roof

For all events, a smooth falling limb, decreasing exponentially, was observed from a nearly saturated roof after various rainfall events (Figure 5). The drainage curves were plotted and processed together with the same starting value. Figure 5 presents the median-observed runoff curve estimated from 14 different events, including the 5th and 95th percentiles. Falling limbs strongly affected by natural rains were excluded from the sample. Additionally, the corresponding relative WC was computed. Even with a minor variation of observed drainage curve, the difference from the 5th percentile to the 95th percentile led to significant variations when computing WC. The WC used with performance indicators was computed based on raw data; hence, while any instability of WC computing should not affect the results presented here, it does highlight the sensitivity of the water balance during long-term events. The WC curve suggests that the detention time is long: starting with 60 mm of WC, it took 3 hours to drain 50% of the water and 6 hours to drain 66% of the water. The analysis

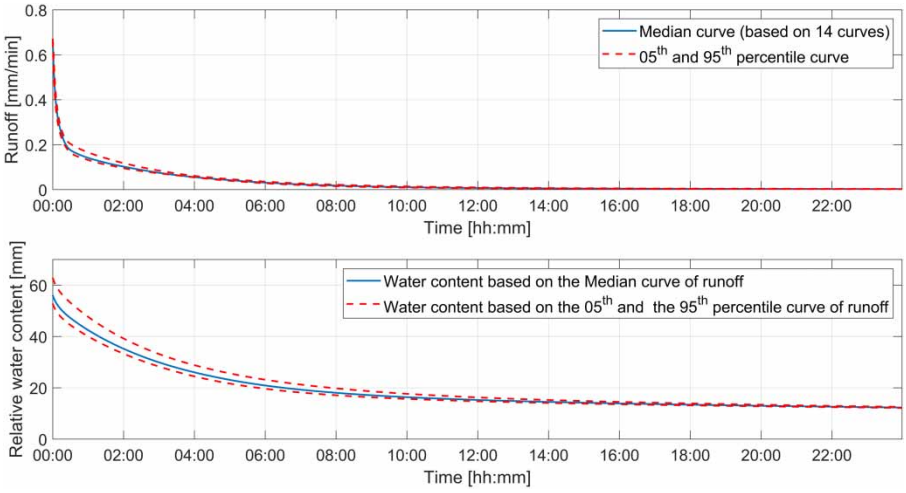

Figure 5 | Median-observed drainage curve for the green roof with 5th and 95th percentile.

Blue-Green Systems Vol 2 No 1
doi: 10.2166/bgs.2020.101

of the dynamic distribution of water within the roof and the hypothesis of a dual porosity of the roof material suggests a relevant explanation to interpret the roof drainage curve. The standing water was drained during the first hour, inducing a quick change of outflow. During the second phase, the outflow had smaller variations as the runoff was driven by its exchange with inner WC (i.e. water in the aggregate). The roof has a long saturation and inner porosity drainage time. Therefore, the previous day rainfall and the corresponding detained water can have a significant influence on the roof performance. Based on this it was chosen to run short events several times per day to experience a range of WC during the experiments second and third steps.

Sensitivity to hyetograph

The hydrological performance of the roof as a source control may be explained and understood using a variety of indicators, as can be seen in (Table A3 and Table A4). When the IWC was low (e.g. lower than field capacity), a plateau of runoff occurred (Figure 6). Consequently, it was not possible to close the event's mass balance, which might slightly alter some indicators. The five artificial events (Table 1

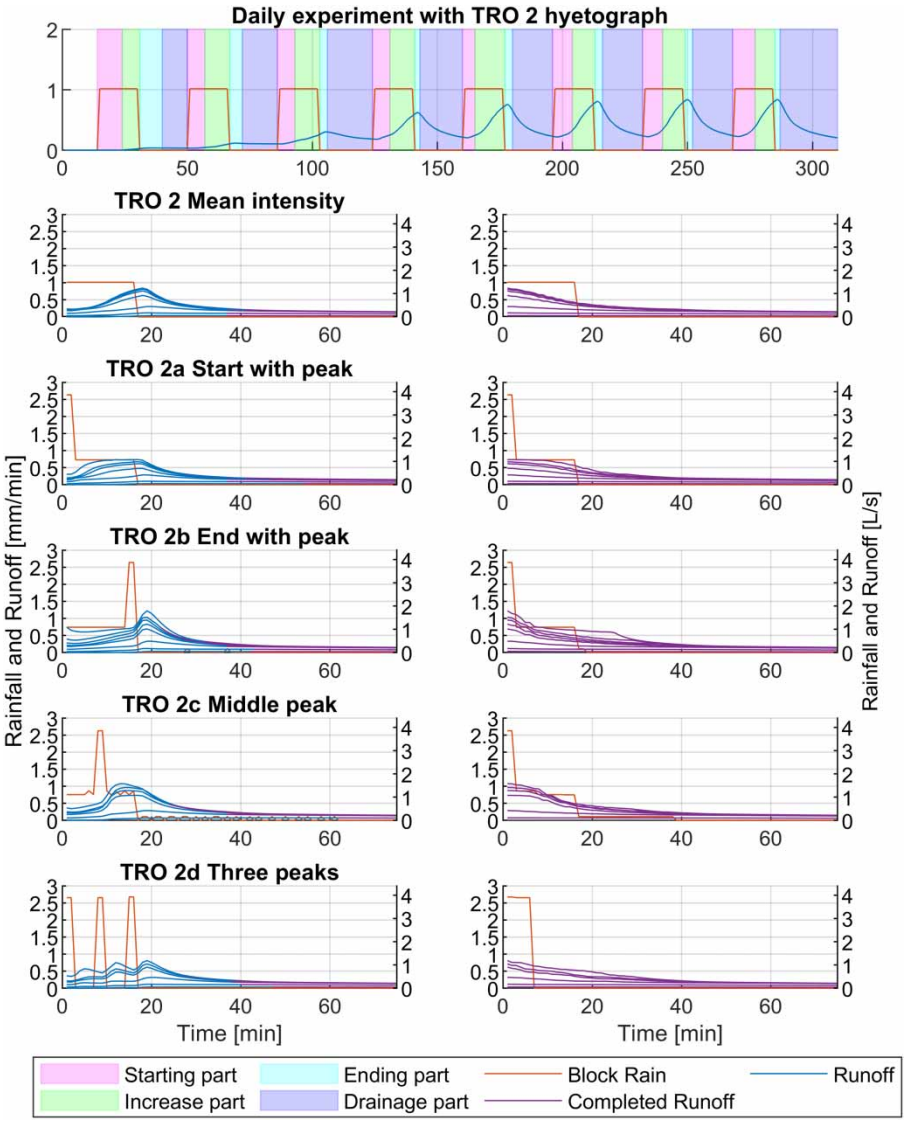

Figure 6 | Comparison of event flow duration for several artificial rainfalls and runoffs for the green roof after 16:00-min blocks with 1.0 mm/min intensity. Mean rainfall depth = 15.9 mm and std = 0.5 mm for all 35 runs.

Blue-Green Systems Vol 2 No 1
doi: 10.2166/bgs.2020.101

and Table A3) chosen to study the influence of the hyetograph shape on the runoff hydrograph were plotted and compared (Figure 6). Table 2 shows the roof initial condition, which is represented by starting outflow and starting relative water content (soil moisture), both of which were found to be important for the performance of the roof. As the peak runoff rose, the roof performance deteriorated with respect to the peak attenuation, T50, centroid delay, and peak delay. The performance of each artificial rain cannot be compared directly without considering these initial conditions.

The green roof was tested using different hyetographs (Figure 6). Absolute values of runoff increased in proportion with increasing IWC. Similarly, a dependency between the initial runoff and peak runoff was found. Running different hyetographs enabled the identification of the sensitivity of the roof. As shown in Figure 6, the position of the peak at the end (TRO 2b) of the rainfall had a large impact on the green roof performance. Following TRO 2b, the green roof generated higher and steeper peak outflows than following TRO2 a, c, d or e. Regarding event flow duration, one can easily read the duration of runoff above a threshold and compare this with the hyetograph. For example, only hyetographs peaking in the middle (TRO 2c) and at the end (TRO 2b) generated runoff from the roof that was greater than 1 mm/min.

There are four observable parts in each runoff hyetograph (illustrated with shaded area on Figure 6):

- the start, a transient state influenced by rainfall (a sudden change of the runoff's gradient);
- the increase, a steady state of the gradient influenced by rainfall;
- the end, a transient state after rainfall stopped that is linked to the dynamic water distribution in both the roof and peak delay (a drop of the gradient);
- the drainage, a steady state of the gradient not influenced by rainfall.

The gradient of the runoff changed smoothly under constant rainfall or without rainfall. Between two stable stages, the gradient changed abruptly: it is the transient stage. The duration of the transition was influenced by the size of the roof and the IWC.

The three indicators selected to assess the effect of the hyetographs are shown in Figure 7. Similarly to previous research (Villarreal & Bengtsson 2005; Li & Babcock 2014; Locatelli *et al.* 2014), there

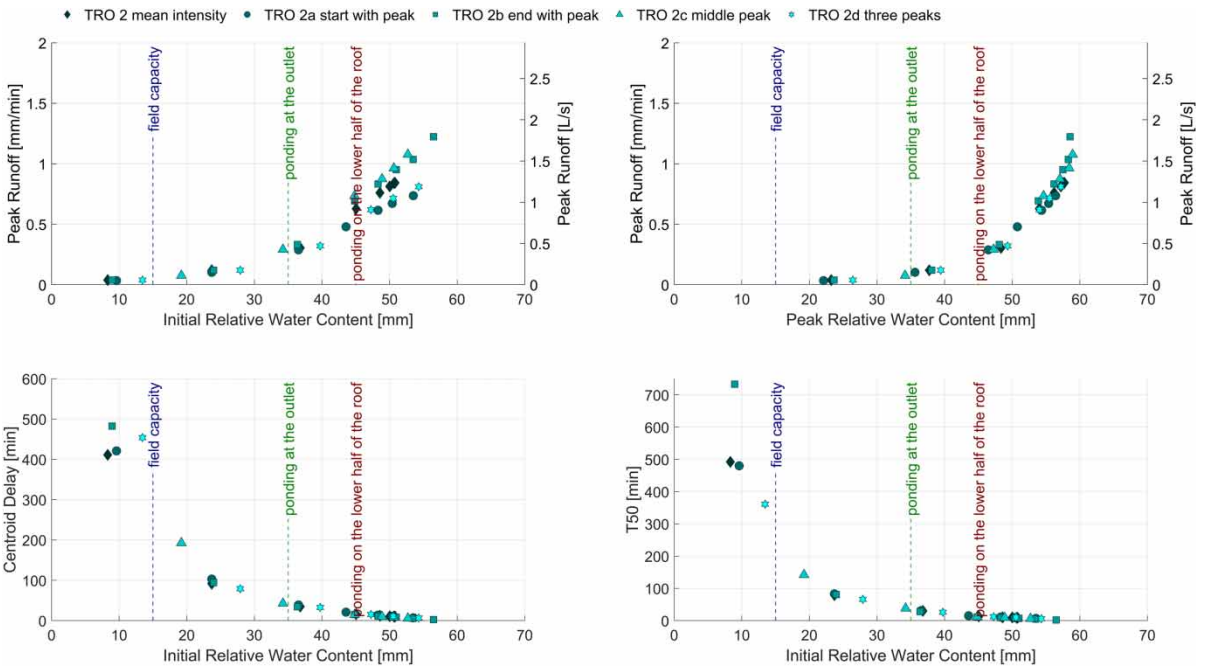

Figure 7 | Observed peak runoff versus IWC and peak relative WC, and centroid delay versus IWC for different hyetographs.

Blue-Green Systems Vol 2 No 1
doi: 10.2166/bgs.2020.101

was a relationship between IWC and peak runoff. Given the same IWC, having the peak at the end (TRO 2b) or in the middle of the rainfall (TRO 2c) event caused higher peak runoff. However, the relationship between the peak runoff and peak relative WC was not notably influenced by the hyetograph. The same conclusion may be drawn by analysing centroid delay in comparison with the IWC. Centroid delay, representing the delay between the centres of mass of rainfall and runoff, was not sensitive to the shape of the hyetographs.

Sensitivity to the rainfall duration and intensity

It was concluded from the second step that the IWC had a stronger influence on performance than the shape of short-term rainfall. Therefore, in order to investigate the roof sensitivity to the rainfall intensity and duration, constant intensity events were studied. Events were chosen based on the 20-year RP IDF curves to ensure realistic values and facilitate a comparison between rainfall events. It should be noted that both future 20-year RP events for Oslo were larger or equal to 200-year RP events under current conditions in Trondheim and Bergen. The roof provided a peak attenuation higher than 93% with the exception of OSL 2. It strengthened the roof's resilience and the capacity to handle a short duration 20-year return period rain in a future climate.

The events corresponding to the Oslo curve generally generated higher runoffs with respect to IWC than events from Bergen and Trondheim (Figure 8). High IWC caused the peak runoff to be close to the peak rainfall. However, when specifically considering the low IWC, the roof was more sensitive to longer rainfalls with lower intensity (e.g. OSL 1 performed worse than OSL 2 with IWC lower than field capacity). The roof with a high starting IWC was more vulnerable to shorter events with higher intensity (e.g. OSL 1 performed better than OSL 2 with IWC higher than 30 mm). Although the same analysis could have been done with OSL 2 and BER 1, or BER 1 and BER 2, the shift appeared with a higher WC (50 mm). Consequently, the roof is sensitive to different short-duration rainfalls depending on its initial condition. Thus, in addition to the DDF curves, the design should be location specific, and based on different events depending on a range of IWC.

Comparing the last artificial rains for TRO 1 and TRO 2 with 50 mm WC, it is noticeable that the peak runoffs were very similar (Table A4, Figure 8). However, the peak attenuation remained very different, showing 50% for TRO 1 and 17% for TRO 2. Moreover, similar observations could be

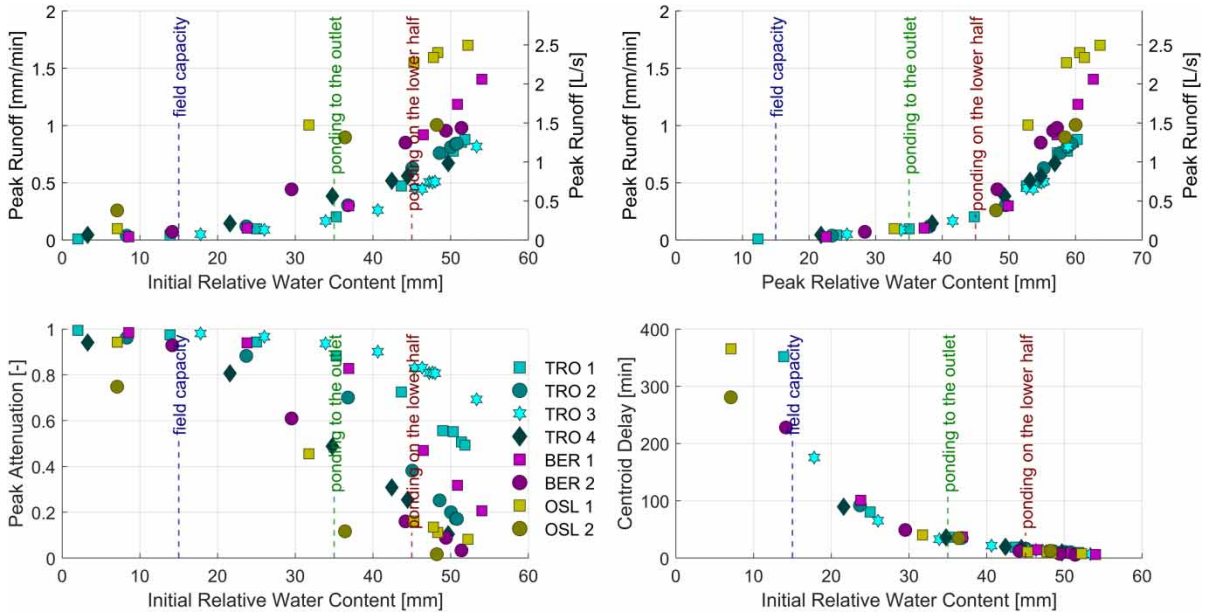

Figure 8 | Comparison between peak runoff, peak attenuation and centroid delay for different locations, including the 1.4 CF.

Blue-Green Systems Vol 2 No 1
doi: 10.2166/bgs.2020.101

done for TRO 2 and TRO 2 a b c d (Table A3). For TRO 2 and TRO 2 a b c d that had the same rainfall depth, but different hyetographs; comparable peak runoffs were found, but the attenuation remained different. Thus, even though peak reduction is a popular performance indicator, it should be presented carefully.

Peak runoff against peak relative WC followed an exponential tendency independent of the type of artificial rain. However, a scattering of peak runoffs was observed with a high peak of relative WC (over 45 mm, with ponding in the middle of the roof), which could be explained by the dynamic spatial distribution of water within the roof. This scattering effect is governed by the mean intensity of previous intervals (i.e. considering previous artificial rain and dry periods). If the roof had not been saturated, a high mean intensity prior to an artificial rain led to a more curved distribution of water within the roof, i.e. to a higher peak runoff than the other events having the same peak relative WC. OSL 2 was the event with the most significant rainfall depth, and thus, it also had the longest inter-event period. This led to smaller dynamic effect, resulting in a steady water distribution across the roof. On the contrary, OSL 1 and BER 2, due to shorter inter-event durations (and to a pipe disconnection during one of the BER 2 tests), underwent more intense antecedent rainfall, which explains why the scatter effect is more noticeable.

The centroid delay in contrast to initial relative WC may be separated into two domains. Having an IWC lower than field capacity, the centroid delay was over 200 minutes. The centroid delays having IWC at field capacity were independent of the rainfall intensity and duration. When the IWC ascended from field capacity (of approximately 15 mm) to 55 mm, the centroid delay decreased by an exponential decay from 200 min to between 5 and 10 minutes, which showed that even a nearly saturated roof outperformed the black roof. Comparable results were found using the T50 delay, which means that the hyetograph, intensity, and duration do not influence centroid delay or T50 delay, i.e. the performance only depends on the IWC.

Performance depending on location

Events linked to Oslo lead to worst performance as their characteristics are more intense than Trondheim or Bergen events. Nevertheless, the performance of the roof depends to a large extent on the IWC. To assess the performance of the roof under a given location those aspects shall be considered. The IWC depends on the climate, i.e. the number and succession of events and the temperature are supposed to greatly influence those parameters. There are more warm days in Oslo than in Trondheim or Bergen. Consequently, a higher Potential Evapotranspiration (PET) is expected in Oslo, even though limited in Nordic climates evapotranspiration is expected to influence the IWC. Moreover, the PET is likely to rise with temperature increase (Hanssen-Bauer *et al.* 2017). The number of rainy days per year and annual precipitation were found for each location: Bergen (205 $\pm$ 18 days, 2,715 $\pm$ 450 mm), Oslo (122 $\pm$ 15 days, 861 $\pm$ 146 mm) and Trondheim (174 $\pm$ 14 days, 1,191 $\pm$ 184 mm) according to the Norwegian Meteorological Institute (https://www.met.no/). This shows that initial conditions are likely to change according to each location. This also means that it is necessary to know the IWC conditions to assess future roof performance.

The worst performance of a short-term artificial rainfall (with <45 min for all the rainfalls) linked to the DDF curves of Oslo does not mean that a higher peak is likely to occur in Oslo than in Bergen. According to the number of days with rainfall, the IWC is expected to be higher in Bergen and Trondheim than in Oslo. However, defining a rainfall with a 6-hour antecedent dry weather period, the initial relative WC could not be higher than 25 mm due to the roof's characteristics (Figure 4). A more realistic initial condition would be to consider one that is less than 20 mm. When initial conditions are between field capacity and 20 mm of WC, the roof's performance would be slightly worse in Oslo than in Bergen for short-term rainfalls. It appeared that OSL 2 (0.25 mm/min peak runoff), with initial conditions lower than field capacity, led to worse performance than TRO 1, 2,

Blue-Green Systems Vol 2 No 1
doi: 10.2166/bgs.2020.101

3, and 4 with 20 mm of IWC (less than 0.15 mm/min peak runoff). Nonetheless, it did not perform significantly worse than BER 1 and 2 with 20 mm of IWC. In this case, the peak runoff would depend more on the characteristics of the hyetograph than on the location. The centroid delay does not depend on the hyetograph and is likely to be higher in Oslo (more than 200 min) with lower initial conditions than in Bergen (between 200 and 100 min). Nevertheless, these expectations only consider short-term rainfalls up to 45 min. Understandably, 20-year return period events are likely to be more intense in Bergen than in Oslo, having a duration over 140 minutes. This study does not conclude about long duration rainfalls, which occur more often in Bergen and Trondheim than in Oslo. The hyetograph was not significant in comparison to the IWC with short-term rain. Nevertheless, it would affect a long duration rain.

CONCLUSION

In this study, a method to test extreme precipitation on a full-scale detention-based green roof consisting of sedum mats underlaid with expanded clay was developed using an artificial rainfall simulator. Rainfall events with 20-year return periods, including a climatic factor of 1.4, were derived from DDF curves for three different cities: Bergen, Oslo, and Trondheim, and tested at the field station in Trondheim. This multistep method that compares different variables depending on the previous steps was found relevant to analyse the global performance of the roof.

The assessment of the hydrological performance showed that retrofitting the black roof as a green roof increased the performance significantly. Furthermore, the roof was found to be sensitive to water content strengthened by long drainage and time of concentration. The study also strengthened the understanding of dynamic phenomena governing the flow within the roof and the limitations that are linked to the use of artificial rainfalls. The use of a various short-term hyetographs led to different roof performance. It was found that the hyetographs with a peak at the end caused the worst performance, and that the initial water content had a greater influence on the performance than the shape of the hyetograph. Considering water content as a main variable, an indicator such as centroid delay that depends on the initial relative water content is suitable for characterizing the roof without depending on the hyetograph. Indeed, the lower the initial water content was, the longer the detention was observed.

With respect to the general performance of the roof and considering initial conditions according to the location, it was possible to assess that the same roof would perform better in Trondheim than in Oslo. It was also found that rainfall in Bergen (BER 1 and 2, with a higher initial water content) and Oslo (OSL 1 and 2, with lower initial water content) is likely to lead to similar peak runoff. Consequently, initial conditions need to be taken into account for design purposes as a more favourable hyetograph may be counterbalanced by a high initial water content. This study has highlighted the relevance of using performance indicators as a function of input parameters instead of using a single-value performance indicator and discussing commonly used indicators. Based on these results, further study is needed to provide statistics to extend the results to longer lasting rainfalls and make generalizations about locations using modelling.

ACKNOWLEDGEMENTS

The study was supported by the Klima2050 Centre for Research-based Innovation (SFI) and financed by the Research Council of Norway and its consortium partners (grant number 237859/030).

Blue-Green Systems Vol 2 No 1
doi: 10.2166/bgs.2020.101

DECLARATION OF INTERESTS

None.

DATA AVAILABILITY STATEMENT

All relevant data are included in the paper or its Supplementary Information.

REFERENCES

Arnbjerg-Nielsen, K. *et al.* 2013 Impacts of climate change on rainfall extremes and urban drainage systems: a review. *Water Science and Technology* **68** (1), 16–28.

Bengtsson, L. 2005 Peak flows from thin sedum-moss roof. *Hydrology Research* **36** (3), 269–280.

Berndtsson, J. C. 2010 Green roof performance towards management of runoff water quantity and quality: a review. *Ecological Engineering* **36** (4), 351–360.

BIPM, I., IFCC, I., ISO, I., IUPAP, O. 2009 Evaluation of measurement data- an introduction to the 'Guide to the expression of uncertainty in measurement' and related documents. *JCGM* **104**, 1–104.

Copenhagen, C. o. 2011 *Copenhagen Carbon Neutral by 2025, Copenhagen Climate Adaptation Plan*.

Dyrrdal, A. V. & Førland, E. J. 2019 *Klimapåslag for korttidsnedbør – Anbefalte verdier for Norge, Norwegian Climate Service Center*.

Fassman-Beck, E., Voyde, E., Simcock, R. & Hong, Y. S. 2013 4 living roofs in 3 locations: does configuration affect runoff mitigation? *Journal of Hydrology* **490**, 11–20.

Few, R. 2003 Flooding, vulnerability and coping strategies: local responses to a global threat. *Progress in Development Studies* **3** (1), 43–58.

FLL 2008 *Guidelines for the Planning, Construction and Maintenance of Green Roofing: Green Roofing Guideline*. Forschungsgesellschaft Landschaftsentwickung Landschaftsbau, Landscape, Research, Development & Construction Society, Bonn, Germany.

Hamouz, V. & Muthanna, T. M. 2019 Hydrological modelling of green and grey roofs in cold climate with the SWMM model. *Journal of Environmental Management* **249**, 109350.

Hamouz, V., Lohne, J., Wood, J. R. & Muthanna, T. M. 2018 Hydrological performance of LECA-based roofs in cold climates. *Water* **10** (3), 263.

Hanssen-Bauer, I. *et al.* 2017 *Climate in Norway 2100 – A Knowledge Base for Climate Adaptation*. Norsk klimasenter.

Hettiarachchi, S., Wasko, C. & Sharma, A. 2018 *Increase in Flood Risk Resulting From Climate Change in A Developed Urban Watershed-the Role of Storm Temporal Patterns*.

Hoegh-Guldberg, O. *et al.* 2018 *Impacts of 1.5 (C Global Warming on Natural and Human systems*.

Johannessen, B., Muthanna, T. & Braskerud, B. 2018 Detention and retention behavior of four extensive green roofs in three nordic climate zones. *Water* **10** (6), 671.

Johannessen, B. G., Hamouz, V., Gragne, A. S. & Muthanna, T. M. 2019 The transferability of SWMM model parameters between green roofs with similar build-up. *Journal of Hydrology* **569**, 816–828.

Kristvik, E., Kleiven, G. H., Lohne, J. & Muthanna, T. M. 2018 Assessing the robustness of raingardens under climate change using SDSM and temporal downscaling. *Water Science and Technology* **77** (6), 1640–1650.

Kristvik, E., Johannessen, B. G. & Muthanna, T. M. 2019 Temporal downscaling of IDF curves applied to future performance of local stormwater measures. *Sustainability* **11** (5), 1231.

Li, Y. & Babcock, R. W. 2014 Green roof hydrologic performance and modeling: a review. *Water Science and Technology* **69** (4), 727–738.

Lindholm, O. G. *et al.* 2008 Veiledning i klimatilpasset overvannshåndtering. *Rapport* **162**, 2008.

Locatelli, L. *et al.* 2014 Modelling of green roof hydrological performance for urban drainage applications. *Journal of Hydrology* **519**, 3237–3248.

Mentens, J., Raes, D. & Hermy, M. 2006 Green roofs as a tool for solving the rainwater runoff problem in the urbanized 21st century? *Landscape and Urban Planning* **77** (3), 217–226.

Miller, J. D. & Hutchins, M. 2017 The impacts of urbanisation and climate change on urban flooding and urban water quality: a review of the evidence concerning the United Kingdom. *Journal of Hydrology: Regional Studies* **12**, 345–362.

Naves, J. *et al.* 2017 Experimental study of pollutant washoff on a full-scale street section physical model. *Water Science and Technology* **76** (10), 2821–2829.

Naves, J., Anta, J., Puertas, J., Regueiro-Picallo, M. & Suárez, J. 2019 Using a 2D shallow water model to assess Large-Scale Particle Image Velocimetry (LSPIV) and Structure from Motion (SfM) techniques in a street-scale urban drainage physical model. *Journal of Hydrology* **575**, 54–65.

Blue-Green Systems Vol 2 No 1
doi: 10.2166/bgs.2020.101

Speak, A., Rothwell, J., Lindley, S. & Smith, C. 2013 Rainwater runoff retention on an aged intensive green roof. *Science of the Total Environment* **461**, 28–38.

Stocker, T. 2014 *Climate Change 2013: The Physical Science Basis: Working Group I Contribution to the Fifth Assessment Report of the Intergovernmental Panel on Climate Change*. Cambridge University Press.

Stovin, V. 2010 The potential of green roofs to manage urban stormwater. *Water and Environment Journal* **24** (3), 192–199.

Stovin, V., Vesuviano, G. & De-Ville, S. 2017 Defining green roof detention performance. *Urban Water Journal* **14** (6), 574–588.

VanWoert, N. D. *et al.* 2005 Green roof stormwater retention. *Journal of Environmental Quality* **34** (3), 1036–1044.

Villarreal, E. L. & Bengtsson, L. 2005 Response of a Sedum green-roof to individual rain events. *Ecological Engineering* **25** (1), 1–7.

Voyde, E., Fassman, E. & Simcock, R. 2010 Hydrology of an extensive living roof under sub-tropical climate conditions in Auckland, New Zealand. *Journal of Hydrology* **394** (3), 384–395.

Zhou, Q. 2014 A review of sustainable urban drainage systems considering the climate change and urbanization impacts. *Water* **6** (4), 976–992.